Self-assembling of nanovoids in 800-keV Ge-implanted Si/SiGe multilayered structures

P. I. Gaiduk,* A. Nylandsted Larsen, and J. Lundsgaard Hansen
Department of Physics and Astronomy, University of Aarhus, DK-8000 Aarhus C, Denmark

E. Wendler and W. Wesch
Institut für Festkörperphysik, Friedrich-Schiller-Universität Jena, Max-Wien-Platz 1, D-07743 Jena, Germany
(Received 7 October 2002; revised manuscript received 13 February 2003; published 11 June 2003)

We report on the self-assembled formation of spherically shaped voids in a Si/SiGe layered structure after 800-keV Ge ion implantation followed by rapid thermal annealing. The voids are of nanometer size and are solely assembled in thin SiGe quantum wells in the surface region ($<R_p/2$) of the implanted sample. The results are discussed in terms of the separation of the vacancy and interstitial depth profiles attributed to the preferential forward momentum of recoiling Si atoms. The strain situation around the SiGe quantum wells is suggested as a possible reason for the void self-assembling effect.

DOI: 10.1103/PhysRevB.67.235311 PACS number(s): 61.72.Qq, 61.72.Ji, 61.72.Ff, 81.15.Hi

I. INTRODUCTION

Despite the remarkable progress in epitaxial-based technologies during the last decades, e.g., in the manufacturing of quantum-size devices,[1] ion implantation continues to be the major ''front end'' process in semiconductor microelectronics and nanoelectronics for precise and controlled doping of materials.[2–4] Ion implantation has the disadvantage of damaging the crystalline structure resulting in different derived effects such as, e.g., transient enhanced diffusion (TED). TED is known as an effect of a strong dopant redistribution generally due to formation of fast diffusing defect complexes which may incorporate dopant atoms and self-interstitials (I) or vacancies (V).[4–7] TED has strongly motivated research efforts directed to the understanding of the mechanisms of defect formation and evolution in implanted layers. It is now commonly agreed that most of the implantation damage is removed during the first stage of annealing via interstitial-vacancy recombination. After annealing the implanted layer contains excess interstitials. In accordance with the well known ''+1'' model,[8] each implanted atom finally occupies a substitutional lattice site, thus replacing the host atom and producing a self-interstitial, so the number of self-interstitials *is* approximately equal to the implanted dose. This fact is well established and repeatedly proven in the case of keV ion implantation.

However, high temperature annealing of MeV implanted Si samples results in the formation of an additional layer of residual defects located between the surface and the mean range R_p of the implanted ions, mostly close to $R_p/2$.[9] These $R_p/2$ defects manifest themselves mainly through the effective gettering of atomic species.[9] The nature of these defects is not yet known and is under intensive discussion. It has been often assumed in particular that the defects in the surface region are vacancy-related agglomerates (clusters),[9–13] which are formed as a consequence of the preferential forward momentum of recoiling Si atoms.[12–14]

A method for mapping the above point defects/clusters and an investigation of their thermal evolution in implanted Si/SiGe are proposed in this paper. The method utilizes the strain situation around thin quantum well (QW) SiGe layers incorporated into a thick Si layer. The method is based on two phenomena. First, due to compressive strain, SiGe/Si QWs may effectively getter and accumulate V and vacancy-related defects.[15] Second, the SiGe/Si QW layers play the role of a diffusion barrier for I and V. In this case the QW layers may prevent both the transport to the surface and the interaction (annihilation) of I and V, located in excess at R_p and at the surface region, respectively. We suggest that if the SiGe/Si QW layers are repeated periodically, then a conservation of I and V may be achieved in a Si layer located between neighboring QW layers.

II. EXPERIMENTAL PROCEDURE

The samples were grown by solid-source molecular beam epitaxy (MBE) using *e*-beam evaporators for the Si and Ge deposition. Wafers of *p*-type (001) Si were used as substrates. Following the SiO_2 desorption from the surface at 850 °C, a 100-nm-thick Si buffer layer was grown. Subsequently, eight successively repeated stages of MBE deposition at growth rates of 0.2 nm/s were proceeded each including: (a) the growth of 2-nm $Si_{0.5}Ge_{0.5}$/3-nm Si/2-nm $Si_{0.5}Ge_{0.5}$ quantum wells, and (b) the growth of a 100-nm Si layer. To prevent relaxation, the thickness of SiGe layers was chosen much beyond of the critical thickness for relaxation of strained SiGe alloy layers. The growth temperature (550 °C) was controlled using both a pyrometer and a thermocouple, giving temperature accuracy better than about 15°. Rutherford backscattering and channeling (RBS/Ch) spectrometry and transmission electron microscopy (TEM) data showed that the as-grown samples were of excellent crystalline quality and no extended defects, clusters of point defects or dislocations were detected in the whole layer system. The $Si_{0.5}Ge_{0.5}$ QW layers were found to be compressively strained with no indication of any detectable relaxation (not shown). The samples were then implanted with 800-keV Ge ions at room temperature to a dose of 2×10^{14} cm^{-2}. Finally, rapid thermal annealing (RTA) in N_2 or O_2 ambients was performed at temperatures of 750–1050 °C for 30 s. For comparison, samples of pure Si were implanted and annealed at similar conditions. The structures

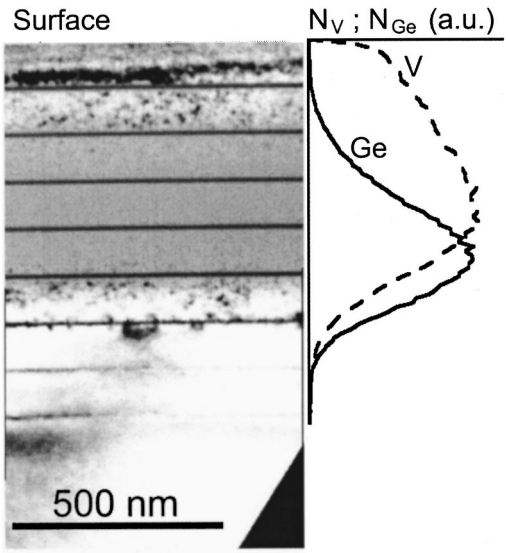

FIG. 1. Bright-field XTEM image of an as-implanted sample with 800-keV 2×10^{14} cm^{-2} Ge ions. The depth profile of Ge and vacancy distribution as obtained by a TRIM95 calculation is reported for comparison. Digits in the image indicate the number of the QW layer from the surface.

were investigated by TEM in both plan-view and cross-section (XTEM) modes using a Philips CM20 instrument operating at 200 kV. The TEM specimens were thinned down to electron transparency using a procedure consisting of successive mechanical polishing and ion-beam milling at room temperature. The samples were also investigated with RBS/channeling spectrometry using a 2-MeV He beam.

III. EXPERIMENTAL RESULTS AND DISCUSSION

Ion implantation of 800-keV Ge at room temperature to a fluence of 2×10^{14} cm^{-2} induces amorphization of the SiGe/Si structure at a depth corresponding to the maximum of the nuclear energy deposition. This is evidenced by the bright field (BF) XTEM image shown in Fig. 1. The implanted sample contains a buried continuous amorphous layer in the depth region between 180 and 560 nm, neighbored by two crystalline, heavily damaged layers at the surface and in the R_p regions. The damaged crystalline layers contain a high concentration of point defect clusters as well as a number of separated amorphous nano-zones located around the amorphous-crystalline interfaces (Fig. 1). The depth profile of the implantation damage is totally disposed inside the QW layer structure, and, thus, the QW layers 1 and 6 (counting from the surface) are located in the crystalline damaged regions, the QW layers 2–5 are in the continuous amorphous zone and the QW layers 7 and 8 are undamaged as are the Si layers surrounding these two QW layers. These XTEM data correlate well with the depth distribution of the nuclear energy deposition. In Fig. 1 the depth profiles of vacancies and implanted Ge as obtained by TRIM95 calculations[16] are included.

RTA at 950 °C for 30 s results in a recrystallization of the buried amorphous layer and the formation of two separated

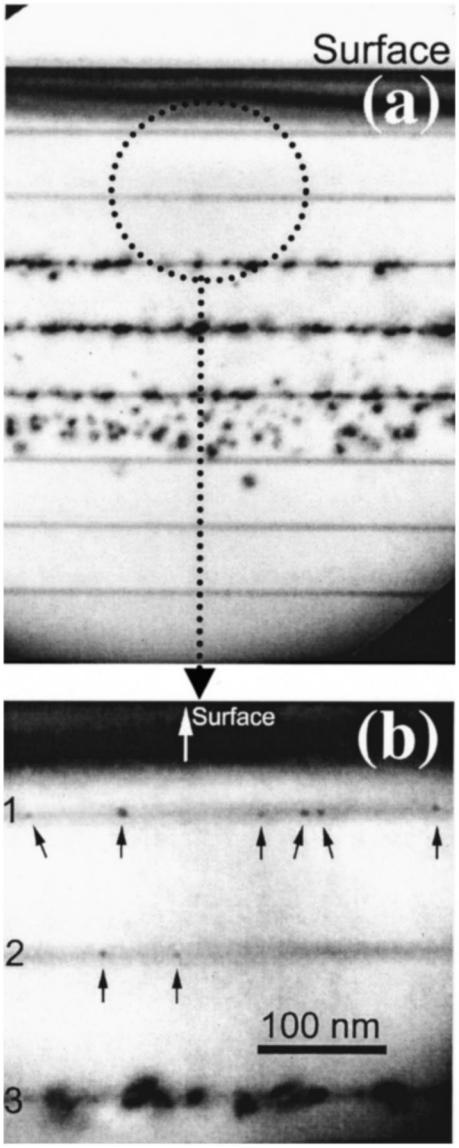

FIG. 2. (a) Focused BF XTEM image of Ge implanted sample after RTA at 950 °C for 30 s in N_2 ambience. (b) Overfocused XTEM image of the surface layer. The arrows in (b) indicate the voids.

bands of extended defects in the R_p region and near to the surface. The interstitial dislocation loops (DLs) are found in the R_p region [Fig. 2(a)], in good agreement with the typical way of thermal defect evolution in implanted Si.[17–19]

A very surprising structural evolution is found near the surface: Neither DLs nor clusters of point defects are observed in the surface region of the sample to a depth of 300 nm. Instead, a number of small (2–6 nm) circular defects are found inside the QW layers 1 and 2 under the out-of-focus regime of the TEM imaging [Fig. 2(b)]. The density of these defects varies between 10^8 and 3×10^{10} cm^{-2}, depending on the thermal treatment. It is also found that the first QW layer (from the surface) contains more defects than the second one and only few circular defects are observed in the third one. The TEM investigations of these defects were carried out in two-beam diffraction conditions with a large deviation pa-

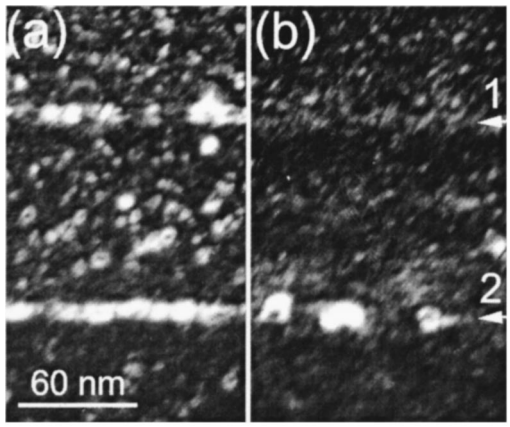

FIG. 3. Dark-field weak-beam XTEM images of Ge implanted sample after RTA at 750 °C (a) and at 830 °C, (b) for 30 s in N_2 ambience. Digits 1 and 2 indicate the position of the first and the second QW layers, respectively.

rameter $s \gg 0$. The defects show minimal contrast at focus. In the underfocused micrograph (not shown) the defects are imaged as bright circles surrounded by Fresnel fringes, whereas in the overfocused micrograph [Fig. 2(b)] they display dark contrast. In dynamical conditions the defects appear as bright against dark regions of the extinction contour, and as dark against bright regions of the extinction contour. The defects keep their circular shape after large inclinations of the sample in the microscope with respect to the electron beam, and they do the same in a cross-section view [Fig. 2(b)]. In accordance with Ref. 20, these observations demonstrate that the circular defects are open-volume defects called voids. We can exclude that these spherical defects are Ge droplets/precipitates from the arguments, similar to presented in Ref. 15.

To clear up the mechanism of this void formation the structural defect evolution was followed as a function of RTA temperature. Figure 3 presents the dark-field weak-beam XTEM micrographs showing the structural defect evolution around QW layers 1 and 2 when the RTA temperature increases. A high density of both small DLs and clusters of point defects is observed in the surface layer after RTA at 750 °C [Fig. 3(a)]. It follows from the TEM analysis at different conditions of image formation[20] that the DLs are of *interstitial* type. An increase of the RTA temperature to 830 °C [Fig. 3(b)] results in a complete removal (around QW layer 1) or a strong decrease of the number (around QW layer 2) of the *interstitial* DLs, preserving, however, a large number of point defect clusters. Taking into account the results of Refs. 10–14 we believe that most of these point defect clusters are *vacancy related*. The bright-field TEM image of such a sample (not shown) displays the formation of a few very small voids inside the QW layer 1 but not yet in the QW layer 2. A further increase of the RTA temperature to 950 and to 1000 °C results in the successive removal of DLs and the formation of voids in the QW layers 2 and 3, respectively, as well as an increase in the density and size of the voids in the QW layer 1. Finally, a further increase of the temperature to 1050 °C results in a partial annealing of the voids. Additionally, it is found from a comparative TEM study of the samples after RTA in oxygen and in nitrogen atmospheres that the oxidation slows down the formation of the voids, especially in the QW layer 1. This can be explained by injection of non-equilibrium self-interstitials during oxidation of Si (Refs. 6 and 7) (also see Ref. 15). Thus it is concluded from the above that a *successive* formation of the *interstitial* DLs and of the (*vacancy-related*) voids takes place in the surface region with *increasing* temperature.

A model based on ballistic separation of Frenkel pairs has been discussed to account for the spatial separation of *V* and *I*, and the vacancy excess within the region around $R_p/2$.[10–14] This model is supported, in particular, by positron annihilation spectroscopy[10–12] and deep level transient spectroscopy (DLTS) measurements,[13] which are able to detect vacancy-related complexes (e.g., vacancy-oxygen (VO) pairs in Ref. 13) or point defect clusters. The thermal evolution of such vacancy related defects is not clear since only interstitial-related {311} defects and DLs are usually observed by TEM after high temperature annealing.[17–19] In the bulk, vacancy-related defects evolve into voids presumably because the activation energy for *V*-type dislocation loop nucleation is one order of magnitude larger than that of nucleating voids; but even in this case the enthalpy is as high as 2.8–3.4 eV, which yields void nucleation temperatures between 970 and 1060 °C.[21] In view of this, a diffusion of excess vacancies from the implanted layer to the surface is energetically a more reasonable path for their removal from the sample. Nevertheless, the formation of voids has been reported recently in Si under special conditions of implantation and annealing. One example is MeV oxygen implants into Si to a high dose,[22] in which case the vacancies are well separated both from interstitials at R_p and from the surface.[9–14] Holland *et al.* reported in Ref. 23 that voids are created in the surface region of Si after extreme conditions (very high dose and temperature) of implantation. Void formation together with Au decoration was also reported in high dose keV implanted samples.[24] Similarly, void formation assisting metallic atom gettering has been demonstrated at a depth of $R_p/2$ in Ref. 9.

Basically, the formation of the voids requires at least vacancy supersaturation in the layer at the temperature of void nucleation. Very fast vacancy migration to the surface at elevated temperatures[6,7] normally prevents vacancy supersaturation in the layers well before the sample reaches the threshold temperature for nucleation of the voids. Note here that only voids of over-critical size are stable and may grow but that the voids of radius smaller than the critical radius shrink in size and disappear.[23,25] Thus, the supersaturation of the vacancies must be high enough to allow the formation of voids of overcritical size. A possible reason of vacancy supersaturation is the formation of large vacancy-related defects (traps) which are stable up to the anneal temperature. The heavily damaged regions which contain, e.g., oxygen[22,23] or metallic[9,23] atoms in high concentration are good candidates for vacancy trapping, for example, due to gettering or segregation effects.[9,22–24] In the present study, however, the accumulation and storage of the vacancies takes obviously place due to the strong nonuniform strain distribu-

tion around the SiGe QW layers. This conclusion is supported by the void assembling within the SiGe QW layers, as can be seen from Fig. 2(b). The as-grown SiGe QW layers are compressively strained before annealing and there is no indication that the layers relax during the subsequent annealing. Thus, the assembly of the voids in the strained SiGe QW layers could be a strain-relieving phenomenon. We believe that in the first stage the vacancy related defects are dissoluted and the vacancies are emitted. A share of the vacancies disappears interacting with interstitial dislocation loops, as can be seen from Fig. 3. Another share of the vacancies, which is in excess of interstitials, diffuses out of the sample. Then the *strain-induced (enhanced)* in-diffusion of vacancies takes place which results in their accumulation in the SiGe QW layers. This is then followed by void nucleation and growth at high annealing temperature.

IV. SUMMARY

In conclusion, a self-assembled formation of voids in a Si/SiGe multilayer structure is observed after Ge ion implantation followed by RTA. The voids are of nanometer size and are solely assembled in thin SiGe QWs in the surface region ($<R_p/2$). The results are discussed in terms of separation of vacancy and interstitial depth profiles. The strain situation around SiGe quantum wells is discussed as a possible reason for the void self-assembling effect.

ACKNOWLEDGMENT

This work was supported by The Danish Strategic Material Research Program.

*Electronic mail: gaiduk@ifa.au.dk

[1] D. Bimberg, M. Grundmann, and N. N. Ledentsov, *Quantum Dot Heterostructures* (Wiley, Chichester, 1999).
[2] J. S. Williams, Mater. Sci. Eng., A **253**, 8 (1998).
[3] J. M. Poate and K. Saadatmand, Rev. Sci. Instrum. **73**, 868 (2002).
[4] E. C. Jones and E. Ishida, Mater. Sci. Eng., R. **24**, 1 (1998).
[5] S. C. Jain, W. Schoenmaker, R. Lindsay, P. A. Stolk, S. Decoutere, M. Willander, and H. E. Maes, J. Appl. Phys. **91**, 8919 (2002).
[6] P. M. Fahey, P. B. Griffin, and J. D. Plummer, Rev. Mod. Phys. **61**, 289 (1989).
[7] S. M. Hu, Mater. Sci. Eng., R. **13**, 105 (1994).
[8] M. D. Giles, J. Electrochem. Soc. **138**, 1160 (1991).
[9] G. A. Rozgonyi, J. M. Glasko, K. L. Beaman, and S. V. Koveshnikov, Mater. Sci. Eng., B **72**, 87 (2000).
[10] B. Nielsen, O. W. Holland, T. C. Leung, and K. G. Lynn, J. Appl. Phys. **74**, 1636 (1993).
[11] S. A. E. Kuna, P. G. Coleman, A. Nejim, F. Cristiano, and P. L. Hemment, Semicond. Sci. Technol. **13**, 394 (1998).
[12] O. W. Holland, J. D. Budai, and B. Nielsen, Mater. Sci. Eng., A **253**, 240 (1998).
[13] P. Pellegrino, H. Kortegaard-Nielsen, A. Hallen, J. Wong-Leung, C. Jagadish, and B. G. Svensson, Nucl. Instrum. Methods Phys. Res. A **186**, 334 (2002).
[14] S. Coffa, V. Privitera, F. Priolo, S. Libertino, and G. Mannino, J. Appl. Phys. **81**, 1639 (1997).
[15] P. I. Gaiduk, J. Lundsgaard Hansen, A. Nylandsted Larsen, and E. A. Steinman, Phys. Rev. B **67**, 235310 (2003).
[16] J. F. Ziegler, J. P. Biersack, and U. Littmark, *The Stopping and Range of Ions in Solids* (Pergamon, New York, 1985).
[17] R. Kögler, A. Peeva, W. Anwand, G. Brauer, W. Skorupa, P. Werner, and U. Gösele, Appl. Phys. Lett. **75**, 1279 (1999).
[18] J. P. Souza, and D. K. Sadana, in *Handbook on Semiconductors* (Elsevier, Amsterdam, 1994), Vol. 30.
[19] K. S. Jones, S. Prussin, and E. R. Weber, Appl. Phys. A: Solids Surf. **45**, 1 (1988).
[20] M. Ruhle and M. Wilkens, Cryst. Lattice Defects **6**, 129 (1975). M. H. Loretto, *Electron Beam Analysis of Materials* (Chapmann and Hall, New York, 1988), p. 210.
[21] P. S. Plekhanov, U. M. Goesele, and T. Y. Tan, J. Appl. Phys. **84**, 718 (1998).
[22] S. L. Ellingboe and M. C. Ridgway, Nucl. Instrum. Methods Phys. Res. B **127**, 90 (1997).
[23] O. W. Holland, L. Xie, B. Nielsen, and D. S. Zhou, J. Electron. Mater. **25**, 99 (1996).
[24] J. S. Williams, M. J. Conway, B. C. Williams, and J. Wong-Leung, Appl. Phys. Lett. **78**, 2867 (2001).
[25] J. Grisolia, A. Claverie, G. Ben Assayag, S. Godey, E. Ntsoenzok, F. Labhom, and A. Van Veen, J. Appl. Phys. **91**, 9027 (2002).